Received: 21 March 2021 | Revised: 10 June 2021 | Accepted: 11 June 2021

DOI: 10.1002/aoc.6347

FULL PAPER

Applied Organometallic Chemistry WILEY

# Synthesis of carbonates from $CO_2$ and epoxides catalyzed by the system of *N*-heterocyclic carbene, hydrogen bond donor, $CrCl_2$, and tetrabutylammonium bromide

**Kuikui Zhang** | **Zhenbang Liu** | **Ning Liu**

School of Chemistry and Chemical Engineering, Key Laboratory for Green Processing of Chemical Engineering of Xinjiang Bingtuan, Shihezi University, Shihezi, Xinjiang, China

**Correspondence**
Ning Liu, School of Chemistry and Chemical Engineering, Key Laboratory for Green Processing of Chemical Engineering of Xinjiang Bingtuan, Shihezi University, North Fourth Road, Shihezi, Xinjiang 832003, China.
Email: ningliu@shzu.edu.cn

**Funding information**
Open Sharing Fund for the Large-scale Instruments and Equipments of Shihezi University; Shihezi Young and Middle-Aged Leading Scientists Program, Grant/Award Number: 2019RC01; Xinjiang Bingtuan Young and Middle-Aged Leading Scientists Program, Grant/Award Number: 2020CB027

**Abstract**

A three-component catalytic system including pyridine-bridged benzimidazolium salts, $CrCl_2$, and tetrabutylammonium bromide (TBAB) was developed. Based on the control experiments and spectroscopic measurements, the role of the three components in the catalytic process was clarified, in which benzimidazolium salts were used as *N*-heterocyclic carbene precursor, a new Cr complex generating from the coordination of $CrCl_2$ with pyridine nitrogen and pyrazole nitrogen bearing benzimidazolium salts was employed as hydrogen bond donor, TBAB was used as nucleophilic reagent, respectively. Under mild conditions (50°C and 1 bar $CO_2$), the terminal epoxides displayed high reactivity in the three-component catalytic system. The catalytic system showed also high catalytic activity for the internal epoxides by increasing the temperature and $CO_2$ pressure and/or prolonging the reaction time.

**KEYWORDS**

carbon dioxide, cooperative catalysis, cyclic carbonate, cycloaddition, epoxide

## 1 | INTRODUCTION

The use of carbon dioxide ($CO_2$) instead of fossil fuels as starting material is a sustainable and renewable alternative for synthesis of chemicals.[1] Therefore, the utilization of $CO_2$ as a carbon feedstock in organic synthesis has attracted wide interest. To date, a number of methods for utilizing $CO_2$ have been developed.[2] The synthesis of cyclic carbonates via the fixation of $CO_2$ have witnessed a significant development in recent years due to the transformation possessing the features of high atomic economy.[3] It is well known that $CO_2$ was the thermodynamically inert and highly kinetically stable molecular; thus, high temperature and high pressure for $CO_2$ in the synthesis of cyclic carbonates is often required. A wide range of strategies employed the metal-mediated catalysts, such as iron,[4] manganese,[5] cobalt,[6] chromium,[7] aluminum,[8] molybdenum,[9] zinc,[10] and magnesium,[11] have been developed for the cycloaddition of $CO_2$ with epoxides, with a focus on achieving catalytic efficiency under mild reaction conditions. In addition, organocatalyzed approaches including imidazolium salts,[12] quaternary ammonium salts,[13] phosphates,[14] and hydrogen bond donors promoted methods,[3c,15] have been demonstrated to a sustainable alternatives for the synthesis of cyclic carbonates.[16] Three-component catalytic systems for the synthesis of cyclic carbonates were summarized in Table 1. Huang and Shi[17] reported an important work for the synthesis of cyclic carbonates using three-component systems composed of NaI/PhOH/$Ph_3P$ (Table 1, entry 1). Werner and co-workers[12c,18] had developed two kinds of

  

**TABLE 1** Comparison of catalytic activity

| Entry | C1 (mol%) | C2 (mol%) | C3 (mol%) | Substrate | T (°C) | $CO_2$ | Time (h) | Isolated yield (%) | TON | TOF ($h^{-1}$) |
|---|---|---|---|---|---|---|---|---|---|---|
| 1[17] | NaI (2) | PhOH (2) | $Ph_3P$ (2) | 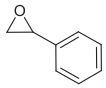 | 120 | 40 bar | 4 | 85 | 42.5 | 10.6 |
| 2[12c] | KI (2) | Carbene (2) | 18C6 (2) | 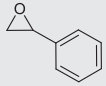 | 100 | 10 bar | 3 | 86 | 43 | 14.3 |
| 3[18] | $CaI_2$ (5) | crown ether (5) | $Ph_3P$ (5) | 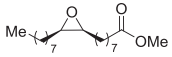 | 45 | 0.5 MPa | 24 | 86 | 17.2 | 0.72 |
| 4[19] | Co $(NO_3)_2$· $6H_2O$ (2) | **L6** (2) | KBr (2) | 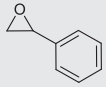 | 100 | 0.6 MPa | 5 | 77 | 38.5 | 7.7 |
| 5 (our work) | $CrCl_2$ (1.5) | **1a** (2) | TBAB (5) | 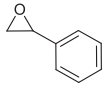 | 50 | 1 bar | 24 | 81 | 40.5 | 1.69 |

*Note*: **C1** = catalytic component 1; **C2** = catalytic component 2; **C3** = Catalytic component 3; TON and TOF calculation based on loading of catalytic component 2 (**C2**).

three-component catalytic systems using KI/carbene/crown ether (Table 1, entry 2) and $CaI_2$/crown ether/$Ph_3P$ (Table 1, entry 3) as catalysts, respectively. Very recently, Wu and Lin[19] reported a catalytic system using $Co(NO_3)_2{\cdot}6H_2O$/hydrogen bond donor/KBr as catalysts (Table 1, entry 4). Although extensively studied, the fixation of $CO_2$ three-component systems remains some significant challenges, including performing in mild reaction temperature and under low pressure for $CO_2$.

In this work, a three-component cooperative catalyzed method for the synthesis of cyclic carbonates had been developed. We expected that the three-component catalytic system had the synergistic effect in which the carboxyl hydrogen bearing Cr complex in situ generating was used as hydrogen bond donor, TBAB acted as a nucleophile, and benzimidazolium salts activated $CO_2$ by forming *N*-heterocyclic carbene (NHC)-adducts. The carboxyl functionalized benzimidazolium salts, used as NHC precursor, reacted with $CO_2$ to form NHC-$CO_2$ adducts, which required extra electron donors to stabilize Cr center. Therefore, we designed and synthesized a pyridine-bridged tridentate ligands base on our research in catalysts design and synthesis.[20] This catalytic system showed wide substrate scope and functional group tolerance under mild reaction conditions (Table 1, entry 5).

## 2 | RESULTS AND DISCUSSION

A series of carboxyl functionalized benzimidazolium salts **1a–f** were synthesized based on our previous literatures.[21] These benzimidazolium salts **1a–f** using as hydrogen bond donors were evaluated in the cycloaddition of epoxides with $CO_2$ (Scheme 1).

The reaction of 1,2-hexylene oxide (**2c**) with $CO_2$ was used as a benchmark reaction to optimize the reaction conditions employing benzimidazolium salts **1a** mentioned above as hydrogen bond donors, metal salts as Lewis acids, and quaternary ammonium salt as nucleophile (Table 2). First, the influence of Lewis acids in catalytic efficiency was investigated (Table 2, entries 1–8), and finding $CrCl_2$ was best effective for the synthesis of cyclic carbonates in 62% yield of **3c** (Table 2, entry 4). The loading amount of $CrCl_2$ was also investigated (Table 2, entries 4 and 9–11), and 1.5 mol% of $CrCl_2$ was appropriate in the view of the cost (Table 2, entry 10).

In the presence of $CrCl_2$ as Lewis acid, the promoted ability of benzimidazolium salts **1a–f** as hydrogen bond donors was also explored (Table 3, entries 1–6), and benzimidazolium salt **1a** displayed the best promoted ability (Table 3, entry 1). The leaving ability of halide anion was in the following order: $I^- > Br^- > Cl^-$. The strong leaving ability of iodine anion was beneficial to generate *N*-heterocyclic carbene $CO_2$ adducts, so that benzimidazolium salt **1a** bearing iodine anion exhibited high performance (Table 3, entry 1). The influences of loading amount of **1a** (Table 3, entries 1 and 7–9) were also evaluated, and it was found that 2 mol% of hydrogen bond donor **1a** was appropriate for achieving 66% yield (Table 3, entry 7). The major function of pyrazole and indazole bearing benzimidazolium salts had a role of ligand for coordinating with Cr center. Therefore,

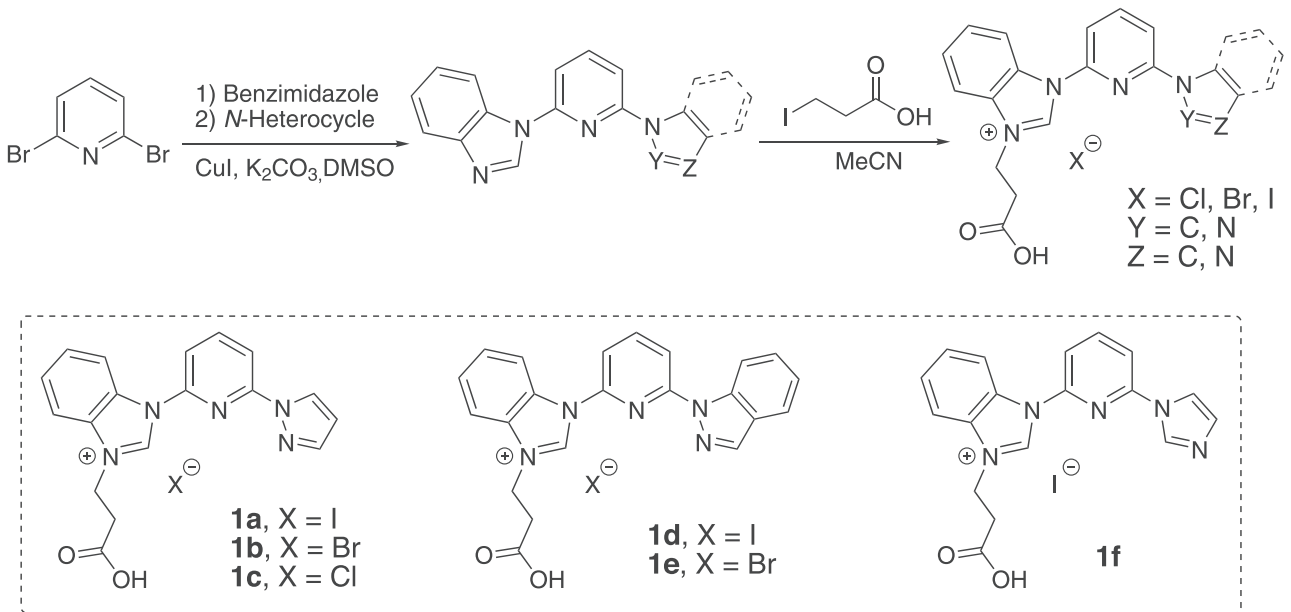


SCHEME 1 The synthesis for carboxyl functionalized benzimidazolium salts

**TABLE 2** Optimization of Lewis acid for cyclic carbonate synthesis

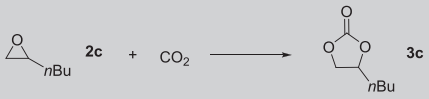


| Entry | Lewis acid (mol%) | Yield (%)[a] | Conversion (%)[b] | Selectivity (%)[b] | TON | TOF ($h^{-1}$) |
|---|---|---|---|---|---|---|
| 1 | $FeCl_2$ (0.5) | 55 | 63 | 99 | 63 | 2.6 |
| 2 | $FeCl_3$ (0.5) | 52 | 59 | 98 | 59 | 2.5 |
| 3 | $CoCl_2$ (0.5) | 45 | 52 | 97 | 52 | 2.2 |
| 4 | $CrCl_2$ (0.5) | 62 | 67 | 99 | 67 | 2.8 |
| 5 | $CrCl_3$ (0.5) | 52 | 59 | 97 | 59 | 2.5 |
| 6 | $ZnCl_2$ (0.5) | 55 | 59 | 96 | 59 | 2.5 |
| 7 | $MnCl_2$ (0.5) | 34 | 40 | 95 | 40 | 1.7 |
| 8 | $MgCl_2$ (0.5) | 35 | 39 | 96 | 39 | 1.6 |
| 9 | $CrCl_2$ (1.0) | 66 | 71 | 99 | 71 | 3.0 |
| 10 | $CrCl_2$ (1.5) | 68 | 73 | 99 | 73 | 3.0 |
| 11 | $CrCl_2$ (2.0) | 69 | 74 | 99 | 74 | 3.1 |

*Note*: Conditions: 1,2-hexylene oxide (5.0 mmol), **1a** (0.05 mmol, 1.0 mol%), Lewis acid (as indicated in Table 2), TBAB (0.1 mmol, 2.0 mol%), 50°C, $CO_2$ balloon (1 bar), 24 h, neat.

[a]Yields were determined by column chromatography.

[b]Conversion and selectivity were determined by GC. TON and TOF were calculated based on the amount of **1a**.

**TABLE 3** Optimization of hydrogen bond donor for cyclic carbonate synthesis

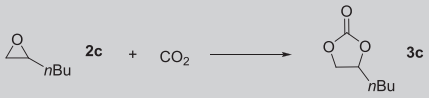


| Entry | Hydrogen bond donor (mol%) | Yield (%)[a] | Conversion (%)[b] | Selectivity (%)[b] | TON | TOF ($h^{-1}$) |
|---|---|---|---|---|---|---|
| 1 | **1a** (1.0) | 62 | 67 | 99 | 67 | 2.8 |
| 2 | **1b** (1.0) | 52 | 60 | 97 | 60 | 2.5 |
| 3 | **1c** (1.0) | 31 | 37 | 93 | 37 | 1.5 |
| 4 | **1d** (1.0) | 41 | 46 | 96 | 46 | 1.9 |
| 5 | **1e** (1.0) | 35 | 39 | 95 | 39 | 1.6 |
| 6 | **1f** (1.0) | 38 | 41 | 93 | 41 | 1.7 |
| 7 | **1a** (2.0) | 65 | 68 | 99 | 34 | 1.4 |
| 8 | **1a** (3.0) | 66 | 71 | 99 | 24 | 1.0 |
| 9 | **1a** (5.0) | 68 | 73 | 99 | 15 | 0.6 |

*Note*: Conditions: 1,2-Hexylene oxide (5.0 mmol), Hydrogen bond donor (as indicated in Table 3), $CrCl_2$ (0.025 mmol, 0.5 mol%), TBAB (0.1 mmol, 2.0 mol%), 50°C, $CO_2$ balloon (1 bar), 24 h, neat.

[a]Yields were determined by column chromatography.

[b]Conversion and selectivity were determined by GC. TON and TOF were calculated based on the amount of hydrogen bond donor.

**TABLE 4** Optimization for cyclic carbonate synthesis

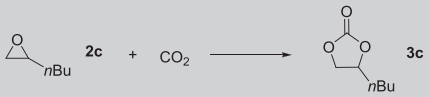


| Entry | Hydrogen bonddonor (mol%) | Lewis acid (mol%) | Nucleophile (mol%) | Yield (%)[a] | Conversion (%)[b] | Selectivity (%)[b] | TON[c] | TOF ($h^{-1}$)[c] |
|---|---|---|---|---|---|---|---|---|
| 1 | **1a** (2.0) | $CrCl_2$ (1.5) | TBAB (3) | 75 | 80 | 99 | 40 | 1.7 |
| 2 | **1a** (2.0) | $CrCl_2$ (1.5) | TBAB (4) | 83 | 86 | 99 | 43 | 1.8 |
| 3 | **1a** (2.0) | $CrCl_2$ (1.5) | TBAB (5) | 89 | 92 | 99 | 46 | 1.9 |
| 4 | **1a** (2.0) | $CrCl_2$ (1.5) | TBAI (5) | 80 | 84 | 99 | 42 | 1.8 |
| 5 | **1a** (2.0) | $CrCl_2$ (1.5) | TBAC (5) | 69 | 73 | 99 | 37 | 1.5 |
| 6 | **1a** (2.0) | $CrCl_2$ (1.5) | TBAO (5) | 70 | 75 | 99 | 38 | 1.6 |
| 7 | **1a** (2.0) | $CrCl_2$ (1.5) | $TBASO_4H$ (5) | 54 | 57 | 99 | 29 | 1.2 |
| 8 | **1a** (2.0) | $CrCl_2$ (0) | TBAB (5) | 39 | 42 | 99 | 21 | 0.9 |
| 9 | **1a** (0) | $CrCl_2$ (1.5) | TBAB (5) | 32 | 34 | 96 | - | - |
| 10 | **1a** (2.0) | $CrCl_2$ (1.5) | TBAB (0) | 10 | 13 | 99 | 7 | 0.3 |
| 11 | **1a** (2.0) | $CrCl_2$ (0) | TBAB (0) | 9 | 14 | 99 | 7 | 0.3 |
| 12 | **1a** (0) | $CrCl_2$ (1.5) | TBAB (0) | 0 | 0 | 0 | - | - |
| 13 | **1a** (0) | $CrCl_2$ (0) | TBAB (5) | 18 | 23 | 95 | - | - |
| 14 | **1a** (0) | $CrCl_2$ (1.5) | TBAB (10) | 42 | 44 | 96 | - | - |
| 15 | **1a** (0) | $CrCl_2$ (1.5) | TBAB (20) | 44 | 47 | 95 | - | - |
| 16[d] | **1a** (0) | $CrCl_2$ (1.5) | TBAB (5) | 70 | 73 | 95 | - | - |
| 17[e] | **1a** (0) | $CrCl_2$ (1.5) | TBAB (5) | 75 | 77 | 96 | - | - |
| 18[f] | **1a** (0) | $CrCl_2$ (1.5) | TBAB (5) | 74 | 78 | 96 | - | - |

*Note*: Conditions: 1,2-Hexylene oxide (5.0 mmol), **1a** (as indicated in Table 4), $CrCl_2$ (as indicated in Table 4), nucleophiles (as indicated in Table 4), 50°C, $CO_2$ balloon (1 bar), 24 h, neat.

[a]Yields were determined by column chromatography.

[b]Conversion and selectivity were determined by GC.

[c]TON and TOF were calculated based on the amount of **1a**.

[d]80°C.

[e]100°C.

[f]$CO_2$ balloon (5 bar).

the coordination ability of pyrazole and indazole was crucial for their catalytic performance. Because the density of electron cloud of indazole tends to benzene ring, the electron-donating properties of indazole was weaker in comparison with pyrazole. Therefore, the pyrazole ring had a stronger coordination ability than that of indazole, which was demonstrated in our previously reported literature.[22] The difference in the catalytic activity between **1a** and **1d** or **1b** and **1e** (Table 3, entries 1 vs. 4 and 2 vs. 5) was caused by the difference in coordination ability between pyrazole and indazole.

The influences for the loading amount of nucleophile tetrabutylammonium bromide (TBAB) (Table 4, entries 1–3) were also evaluated; 5 mol% of TBAB was appropriate for high conversion, and achieving 89% yield (Table 4, entry 3). Besides TBAB, other nucleophiles including tetrabutylammonium iodide (TBAI), tetrabutylammonium chloride (TBAC), tetrabutylammonium acetate (TBAO), and tetrabutylammonium hydrogen sulfate ($TBASO_4H$) were explored under the optimized reaction conditions (Table 4, entries 4–7), and TBAB showed the best performance for the transformation (Table 4, entry 3). Generally, there are two factors affecting the nucleophilic attack process of the nucleophiles, which are the nucleophilic ability and the size of the counterions. The bromide anions had good nucleophilicity and

**TABLE 5** Scope for epoxides

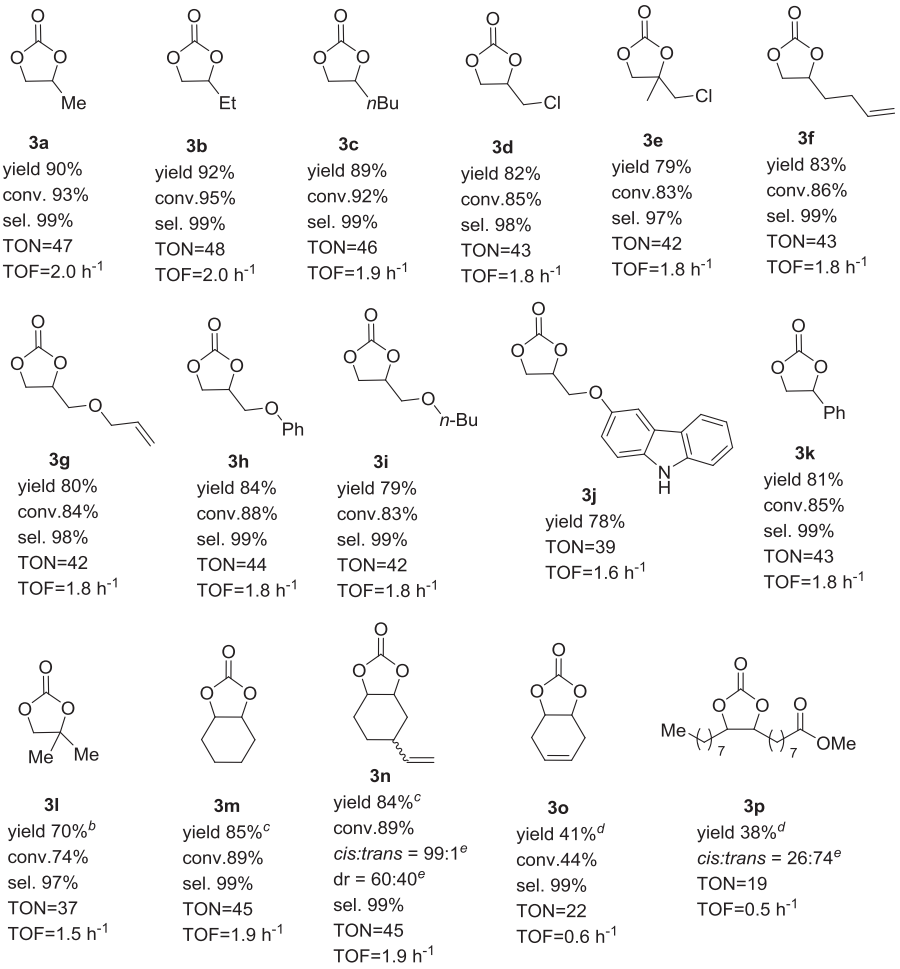


**3a**
yield 90%
conv. 93%
sel. 99%
TON=47
TOF=2.0 $h^{-1}$

**3b**
yield 92%
conv.95%
sel. 99%
TON=48
TOF=2.0 $h^{-1}$

**3c**
yield 89%
conv.92%
sel. 99%
TON=46
TOF=1.9 $h^{-1}$

**3d**
yield 82%
conv.85%
sel. 98%
TON=43
TOF=1.8 $h^{-1}$

**3e**
yield 79%
conv.83%
sel. 97%
TON=42
TOF=1.8 $h^{-1}$

**3f**
yield 83%
conv.86%
sel. 99%
TON=43
TOF=1.8 $h^{-1}$

**3g**
yield 80%
conv.84%
sel. 98%
TON=42
TOF=1.8 $h^{-1}$

**3h**
yield 84%
conv.88%
sel. 99%
TON=44
TOF=1.8 $h^{-1}$

**3i**
yield 79%
conv.83%
sel. 99%
TON=42
TOF=1.8 $h^{-1}$

**3j**
yield 78%
TON=39
TOF=1.6 $h^{-1}$

**3k**
yield 81%
conv.85%
sel. 99%
TON=43
TOF=1.8 $h^{-1}$

**3l**
yield 70%[b]
conv.74%
sel. 97%
TON=37
TOF=1.5 $h^{-1}$

**3m**
yield 85%[c]
conv.89%
sel. 99%
TON=45
TOF=1.9 $h^{-1}$

**3n**
yield 84%[c]
conv.89%
*cis:trans* = 99:1[e]
dr = 60:40[e]
sel. 99%
TON=45
TOF=1.9 $h^{-1}$

**3o**
yield 41%[d]
conv.44%
sel. 99%
TON=22
TOF=0.6 $h^{-1}$

**3p**
yield 38%[d]
*cis:trans* = 26:74[e]
TON=19
TOF=0.5 $h^{-1}$

*Note*: Conditions unless specified otherwise: epoxides (5.0 mmol), **1a** (2 mol %), $CrCl_2$ (1.5 mol%), TBAB (5 mol%), 50°C, $CO_2$ balloon (1 bar), 24 h, neat, Yields were determined by column chromatography. Conversion and selectivity were determined by GC.

[a]80°C.

[b]100°C, 5 bar $CO_2$.

[c]100°C, 5 bar $CO_2$, TBAB (10 mol %), 36 h.

[d]The ratio of *cis*:*trans* and d.r. values were determined by $^1H$ and $^{13}C$ NMR spectroscopy. TON and TOF were calculated based on the amount of **1a**.

moderate size, which promoted the nucleophilic attack to epoxides. The benzimidazolium salt itself contained halogen anions; however, additional halogen anions from TBAB are still required, which can be explained by Caló et al.[23] They had found that the chemical structure and size of the cations bearing quaternary ammonium salts had evident influence in the nucleophilic attack ability of anions. The results indicated that the difference of the cations led to different nucleophilic abilities of the two types of halogen anions, and the halogen anions from TBAB had higher nucleophilic abilities than that of the halogen anions on benzimidazolium salts.[20b] To explore the function of three catalytic components, three control experiments were performed in the absence of $CrCl_2$ or **1a** or TBAB, respectively. Notably, $CrCl_2$, **1a**, and TBAB were necessary for high efficiency, because the absence of any one of them resulted in a remarkable decline in the yield of **3c** (Table 4, entries 8–13 vs. 3). To prove the effect of **1a**, a series of control experiments in the absence of **1a** were performed (Table 4, entries 14–18). When the amount of TBAB increased to 10% or 20% in the absence of **1a**, the yield of the target product increased slightly (Table 4, entries 14 and 15 vs. 3). The increase of reaction temperature and pressure of $CO_2$ effectively promoted this

transformation; however, the result was difficult to achieve the result obtained in the absence of **1a** in the mild conditions (Table 4, entries 16–18 vs. 3). This result indicated that benzimidazolium salt **1a** is essential in this transformation.

Under the optimized conditions obtained above, the scope of epoxides was explored (Table 5). First, a wide range of aliphatic substituted terminal epoxides were used as substrates, and a series of aliphatic mono-substituted cyclic carbonates were obtained in high yields (Table 5, **3a**-**j**). The phenyl substituted terminal epoxides were examined, and producing **3 k** in 81% yield. The 2,2-dimethyloxirane are often challenging substrates. To our delighted, we found that it was also converted to the desired product **3 L** in 70% yield when reaction temperature increased to 80°C.

Internal epoxides such as bicyclic epoxides were particularly challenging substrates and were difficult to convert them into the desired products because of their highly steric hindrance. Therefore, the substrates tolerance of the cyclohexene oxides was explored in the established catalyzed system. Three cyclohexene oxides, including two cyclohexene oxide containing *exo*- or internal-cyclic double bonds, could be converted into

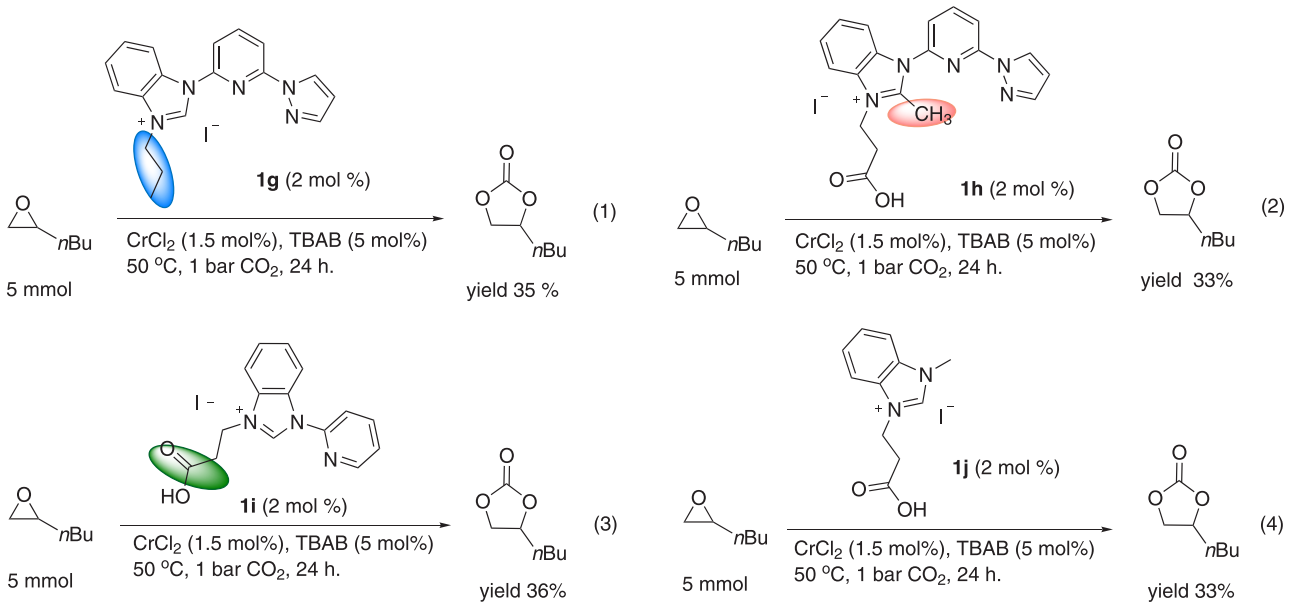


**SCHEME 2** Study on active sites of catalysts

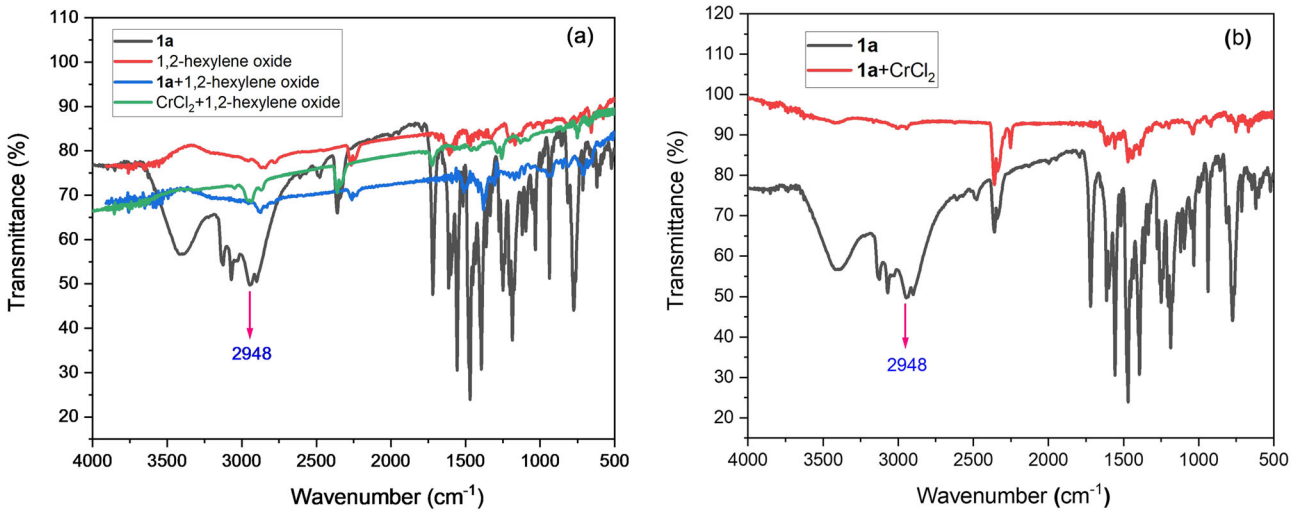


**FIGURE 1** FT-IR spectra for reaction mechanism

their cyclic carbonates **3 m-o** in good yields by increasing reaction temperature, increasing pressure for $CO_2$, and/or loading amount of TBAB and prolonging time. The bio-derived epoxides were high sterically hindered substrates and had a potential application in polymer synthesis. For example, the reaction of epoxidized methyl oleate with $CO_2$ was also converted and a bio-based carbonate **3p** was isolated in 38% yield with a *cis*:*trans* ratio of 26:74.

To clarify the influence of each active sites bearing benzimidazolium salt **1a**, two catalysts were designed to obtain some mechanistic insights into the reaction mechanism (Scheme 2). To explore the effect of carboxyl group bearing **1a**, a catalyst **1g** was synthesized by the replacing of carboxyl group with propyl group. In the replacement of **1a** with **1g** resulted a significant decline in yield from 89% to 35% (Scheme 2, eq 1 vs. Table 4, entry 3). The result suggested that the carbonyl group had played an important role in the catalytic performance.

To demonstrate the role of hydrogen atom at C2 position of **1a** in reaction process, a catalyst **1h** was synthesized by introducing a methyl group to the C2 position of **1a** (Scheme 2, eq 2). The result indicated that the yield obviously decreased from 89% (Table 4, entry 3) to 33% when the C2 position was methylated, in which methylation of the C2 position prevented the interaction between $CO_2$ and active site of the C2 position. Therefore, we inferred that **1a** was used as NHC precursor to activate $CO_2$ through reacted with $CO_2$ to form NHC adducts.

In addition, the function of pyridine ring and pyrazole ring bearing benzimidazolium salt **1a** was explored in Scheme 2. When pyridine ring and pyrazole ring were removed from imidazolium salt **1a** (Scheme 2, eqs 3 and 4), both **1i** and **1j** showed low performance compared with that of **1a**. We inferred that pyridine ring and pyrazole ring had played a role of nitrogen donors to coordinate with $CrCl_2$ to generate a new Cr complex.

To investigate the interaction between **1a** and 1,2-hexylene oxide, several control experiments were performed using FT-IR method. The absorption peak at 2948 $cm^{-1}$ was assigned to the stretching vibration peak of the carboxyl group bearing **1a** (Figure 1a, black curve). When 50 equiv of 1,2-hexylene oxide was added to **1a**, the absorption peak of the carboxyl group disappeared (Figure 1a, blue curve). These changes indicated that the hydrogen bond between the carboxyl group bearing **1a** and 1,2-hexylene oxide may occur.

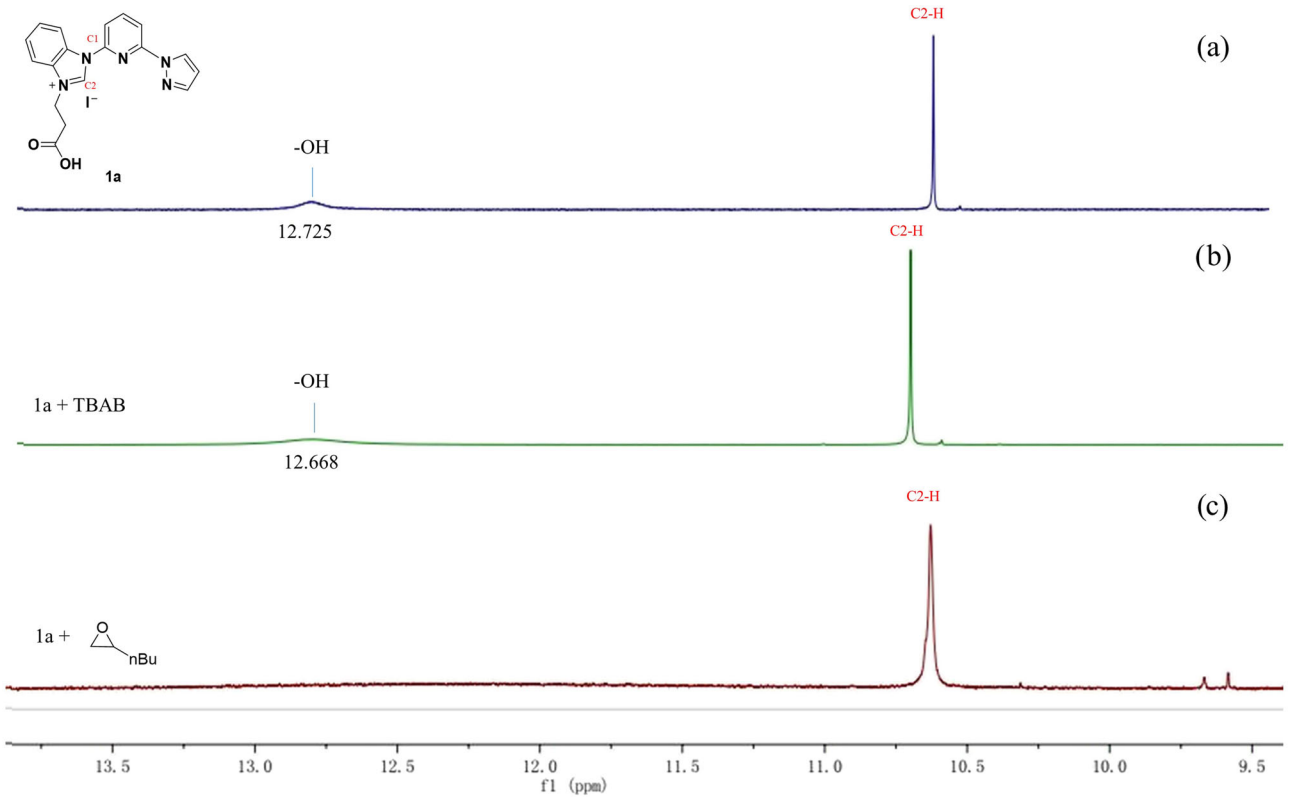


FIGURE 2 $^1$H NMR experiments for the interaction between **1a** and epoxide **2c**

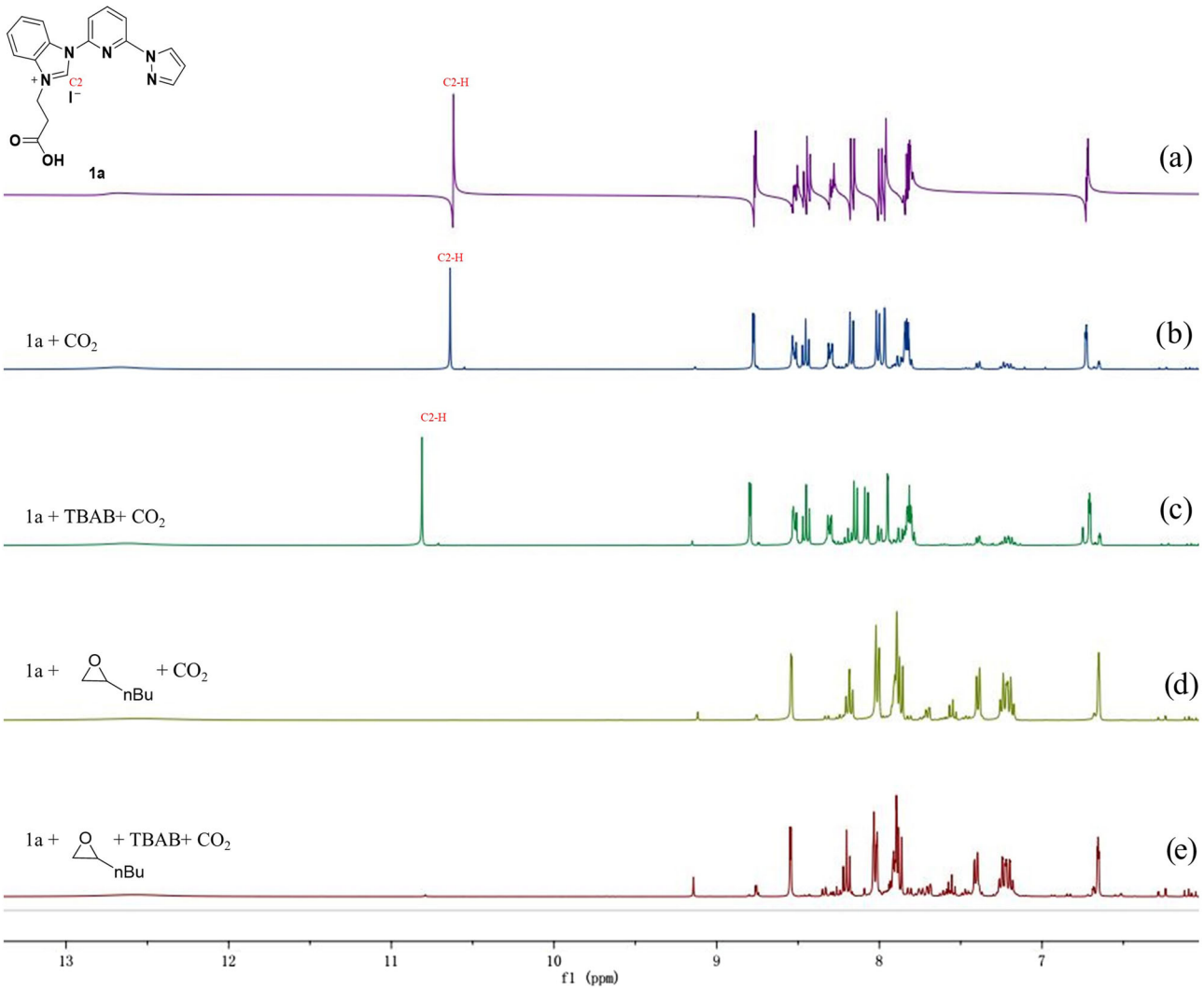


FIGURE 3 $^1$H NMR experiments for the interaction between **1a** and $CO_2$

When $CrCl_2$ was added to 1,2-hexylene oxide, no obvious changes were observed (Figure 1a, green curve), indicating $CrCl_2$ did not act as a Lewis acid. Therefore, we next explored the interaction between **1a** and $CrCl_2$ (Figure 1b). When $CrCl_2$ was added to **1a**, the absorption peaks of the carboxyl group bearing **1a** disappeared (Figure 1b, red curve). This change indicated that the carboxyl group bearing **1a** coordinated with $CrCl_2$ to generate a new Cr complex. This result was consistent with control experiments in Scheme 2 (eqs 3 and 4). Full IR spectra are detailed in Figures S27 and S28.

To prove whether the hydrogen bond interaction between the carboxyl group bearing **1a** and bromide anion of TBAB occurs,[24] three control experiments were performed by NMR method (Figure 2). When TBAB was added to **1a**, the absorption peak of the carboxyl group bearing **1a** had not changed (Figure 2b); however, the addition of 1,2-hexylene oxide led to the disappearance (Figure 2c). These changes indicated that the hydrogen bond interaction between the carboxyl group bearing **1a** and bromide anion of TBAB did not occur; however, the hydrogen bond interaction between the carboxyl group bearing **1a** and oxygen atom of 1,2-hexylene oxide was observed. Full NMR spectra are detailed in Figure S29.

To determine whether the NHC-$CO_2$ adducts via the reaction of C2-H of **1a** with were formed, a wide range of control experiments was performed by $^1$H NMR method (Figure 3). When $CO_2$ and/or TBAB were added to **1a**, the absorption peak of C2-H bearing **1a** had not disappeared (Figure 3a–c); however, the addition of 1,2-hexylene oxide led to the disappearance

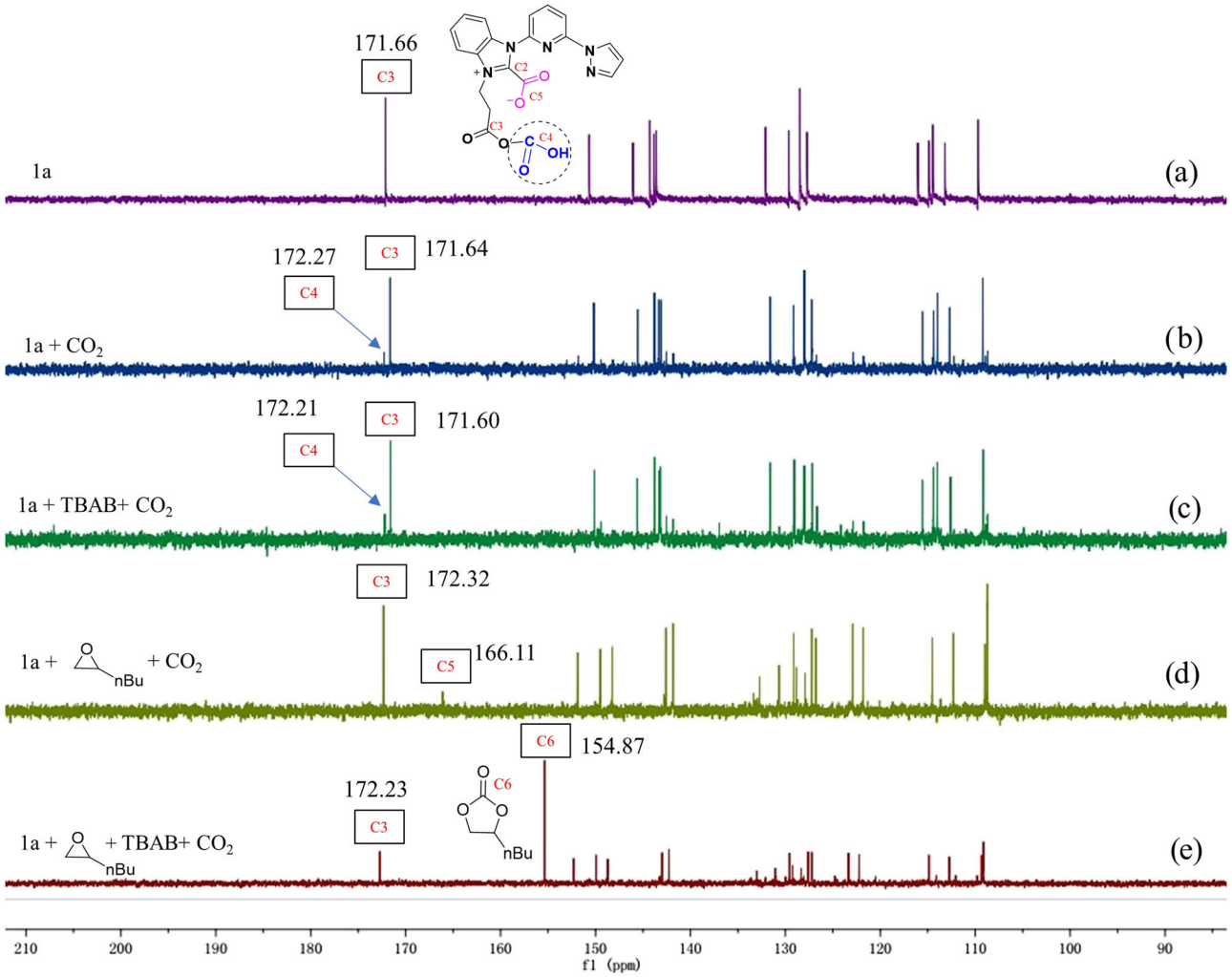


FIGURE 4 $^{13}C$ NMR experiments for the interaction between **1a** and $CO_2$

(Figure 3d,e). These changes indicated that the NHC-$CO_2$ adducts may be formed. In order to confirm the results above, a series of control experiments were performed by $^{13}C$ NMR method (Figure 4). When $CO_2$ and/or TBAB were added to **1a**, a new absorption peak in 172.27 ppm was observed (Figure 4a–c). According to literatures,[25] we inferred that the carboxyl group bearing **1a** reacted with $CO_2$ to generate acid anhydride intermediates. When 1,2-hexylene oxide was added to the reaction mixtures above, a new absorption peak in 166.11 ppm was observed (Figure 4d), and simultaneously acid anhydride intermediates disappeared. The results indicated that NHC-$CO_2$ adducts[26] were produced when $CO_2$ transferred from the carboxyl group to C2 position of **1a**. The NHC-$CO_2$ adducts was disappeared when the desired product **3c** was achieved (Figure 4e). Full NMR spectra are detailed in Figures S30 and S31.

Based on control experiments (Scheme 2) and spectroscopic measurements (IR and NMR in Figures 1 and 2) above, we illustrated the role of $CrCl_2$, benzimidazolium salt **1a**, and TBAB in the catalytic process. As shown in Scheme 3, the carboxyl hydrogen bearing benzimidazolium salt **1a** was used as hydrogen bond donor,[27] and TBAB acted as a nucleophile. The C2 hydrogen at benzimidazolium salt **1a** could react with $CO_2$ to form *N*-heterocyclic carbene adducts,[26,28] which has played a role in activating $CO_2$. As shown in Scheme 3, a new Cr complex **A** generated from the coordination of benzimidazolium salt **1a** with $CrCl_2$ was used as Lewis acid through the hydrogen bond interaction between carboxyl hydrogen and oxygen atom of epoxides. Epoxides underwent continuous ring-opening reaction via intramolecular nucleophilic attack of bromide from TBAB, $CO_2$ insertion reaction, and ring-closure reaction to form target products and release catalytic active species.

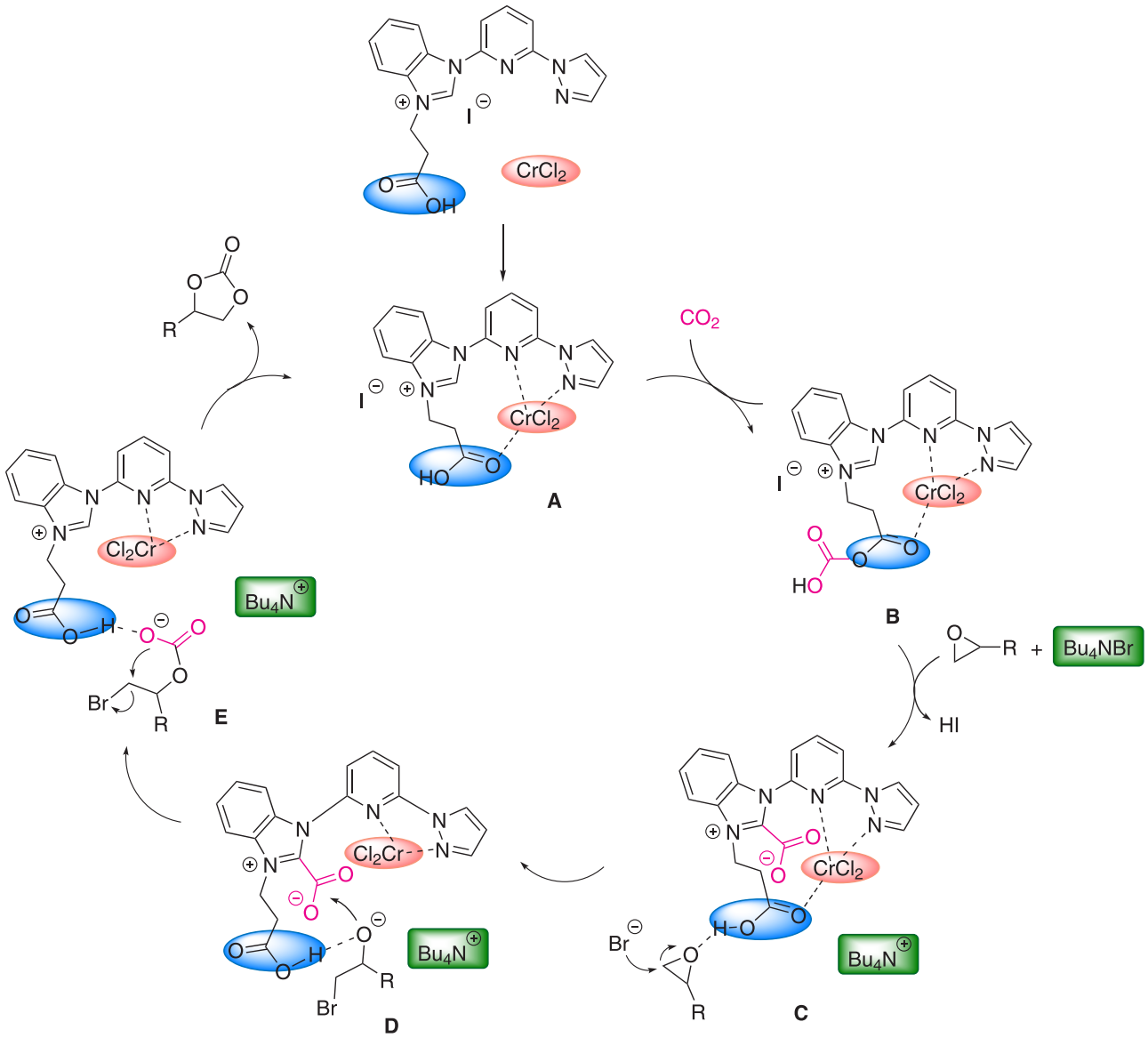


SCHEME 3 Proposed mechanism for the synthesis of cyclic carbonates

## 3 | CONCLUSIONS

In conclusion, an efficient catalytic system was presented to prepare cyclic carbonates through the cycloaddition of epoxides with $CO_2$, which was composed of benzimidazolium salts, $CrCl_2$, and TBAB. The three-component catalytic system showed wide scope of terminal epoxides, as well as internal epoxides with excellent functional group tolerance in high products yield. The role of each component in the catalytic process was explored in the control experiments and spectroscopic measurements. The results indicated that $CrCl_2$ coordinated with benzimidazolium salts to form a new Cr complex as Lewis acids, in which the carboxyl group bearing new Cr complex enhanced the nucleophilic attack of TBAB to open the ring of epoxides by hydrogen bond interaction between carboxyl hydrogen and oxygen atoms with epoxides. The benzimidazolium salts could activate $CO_2$ via the formation of *N*-heterocyclic carbene adducts.

## 4 | EXPERIMENTAL

### 4.1 | Analytical methods

All solvents and reagents were purchased from commercial sources used without additional purification. NMR spectra were recorded on a Bruke Avance III HD 400 spectrometer using TMS as internal standard (400 MHz for $^{1}H$ NMR and 100 MHz for $^{13}C$ NMR). High-resolution mass spectroscopy (HRMS) data were

collected on a Bruker solanX 70 FT-MS and Agilent 6224 TOF mass spectrometer. FT-IR spectra were recorded on Tianjin Gangdong FTIR-650. All products were isolated by flash chromatography on a silica gel (300–400 mesh) column.

## 4.2 | General procedure for the synthesis of benzimidazolium salts

A mixture of 2,6-dibromopyridine (0.5 mmol), benzimidazole (0.75 mmol), CuI (0.1 mmol), and $K_2CO_3$ (1.5 mmol) in DMSO (2 ml) was stirred for 24 h at 90°C under nitrogen atmosphere.[21] The solvent was concentrated under vacuum, and the product of 2-bromo-6-substituent-pyridine was isolated by short chromatography. Thereafter, 2-bromo-6-substituent-pyridine (0.5 mmol), *N*-heterocycle (0.75 mmol), CuI (0.1 mmol), and $K_2CO_3$ (1.5 mmol) in DMSO (2 ml) was allowed to react 48 h at 120°C under nitrogen atmosphere. The solvent was removed under reduced pressure, and the product of pyridine-bridged pincer-type compound was isolated by short chromatography. The pyridine-bridged pincer-type compound (0.5 mmol) and 3-iodopropionic acid (0.7 mmol) were put into a 25-ml Schlenk tube and added 3-ml acetonitrile solvent under a nitrogen atmosphere. The reaction was carried out at 80°C for 24 h. Then, the acetonitrile was evaporated under reduced pressure, and the crude products were purified by silica gel column chromatography using dichloromethane: methanol = 10:1 as eluent.

### 4.2.1 | Benzimidazolium salt **1a**

Purification by flash chromatography (dichloromethane: methanol = 10:1): a yellow solid, mp 194.3°C to 201.5°C; $^1$H NMR (400 MHz, DMSO-$d_6$): $\delta$ 12.73 (s, 1H), 10.62 (s, 1H), 8.76 (d, $J$ = 2.4 Hz, 1H), 8.54–8.50 (m, 1H), 8.45 (t, $J$ = 8.0 Hz, 1H), 8.31–8.27 (m, 1H), 8.16 (d, $J$ = 8.4 Hz, 1H), 8.00 (d, $J$ = 7.6 Hz, 1H), 7.96 (d, $J$ = 1.2 Hz, 1H), 7.85–7.80 (m, 2H), 6.72 (dd, $J$ = 2.4 Hz, $J$ = 1.6 Hz, 1H), 4.84 (t, $J$ = 7.2 Hz, 2H), 3.14 (t, $J$ = 7.2 Hz, 2H). $^{13}$C NMR (100 MHz, DMSO-$d_6$): $\delta$ 171.66, 150.20, 145.58, 143.82, 143.38, 143.14, 131.62, 129.17, 128.02, 127.25, 115.58, 114.40, 114.00, 112.73, 109.23, 43.14, 32.85. IR (KBr) 3393, 2944, 1710, 1610, 1557, 1466, 1390, 1253, 1192, 1017, 933, 780 cm$^{-1}$. HRMS: (ESI-TOF), $m/z$ calcd.: 334.1299 for $C_{18}H_{16}N_5O_2$; found: 334.1292 $[M - I]^+$. The NMR spectra and FT-IR spectra of benzimidazolium salt **1a** can be found in Figures S1 and S32.

### 4.2.2 | Benzimidazolium salt **1b**

Purification by flash chromatography (dichloromethane: methanol = 10:1): a yellow solid, mp 196.7°C to 201.2°C; $^1$H NMR (400 MHz, DMSO-$d_6$): $\delta$ 10.79 (s, 1H), 8.78 (d, $J$ = 2.4 Hz, 1H), 8.52–8.50 (m, 1H), 8.43 (t, $J$ = 8.0 Hz, 1H), 8.29–8.27 (m, 1H), 8.13 (d, $J$ = 8.0 Hz, 1H), 8.06 (d, $J$ = 7.6 Hz, 1H), 7.94 (s, 1H), 7.83–7.77 (m, 2H), 6.70 (t, $J$ = 1.6 Hz, 1H), 4.85 (t, $J$ = 6.8 Hz, 2H), 3.11 (t, $J$ = 6.8 Hz, 2H). $^{13}$C NMR (100 MHz, DMSO-$d_6$): $\delta$ 171.97, 150.10, 145.63, 143.75, 143.30, 143.17, 131.60, 129.06, 128.10, 127.97, 127.19, 115.61, 114.42, 113.96, 112.59, 109.18, 43.40, 33.32. IR: (KBr) 3340, 2959, 1725, 1619, 1550, 1474, 1397, 1245, 1184, 1032, 933, 742 cm$^{-1}$. HRMS: (ESI-TOF), $m/z$ calcd.: 334.1299 for $C_{18}H_{16}N_5O_2$; found: 334.1294 $[M - Br]^+$. The NMR spectra and FT-IR spectra of benzimidazolium salt **1b** can be found in Figures S2 and S33.

### 4.2.3 | Benzimidazolium salt **1c**

Purification by flash chromatography (dichloromethane: methanol = 10:1): a yellow solid, mp 199.1°C to 204.7°C; $^1$H NMR (400 MHz, DMSO-$d_6$): $\delta$ 10.91 (s, 1H), 8.79 (d, $J$ = 2.8 Hz, 1H), 8.53–8.51 (m, 1H), 8.42 (t, $J$ = 8.0 Hz, 1H), 8.30–8.28 (m, 1H), 8.14 (d, $J$ = 8.0 Hz, 1H), 8.07 (d, $J$ = 8.0 Hz, 1H), 7.94 (d, $J$ = 0.8 Hz, 1H), 7.84–7.78 (m, 2H), 6.71 (t, $J$ = 2.0 Hz, 1H), 4.85 (t, $J$ = 6.8 Hz, 2H), 3.17 (t, $J$ = 6.8 Hz, 2H). $^{13}$C NMR (100 MHz, DMSO-$d_6$): $\delta$ 171.63, 150.18, 145.70, 143.78, 143.36, 131.66, 129.14, 128.12, 127.98, 127.21, 115.64, 114.43, 113.99, 112.65, 109.22, 43.13, 33.04. IR: (KBr) 3340, 2989, 1733, 1619, 1557, 1474, 1397, 1253, 1192, 1032, 940, 742 cm$^{-1}$. HRMS: (ESI-TOF), $m/z$ calcd.: 334.1299 for $C_{18}H_{16}N_5O_2$; found: 334.1307 $[M - Cl]^+$. The NMR spectra and FT-IR spectra of benzimidazolium salt **1c** can be found in Figures S3 and S34.

### 4.2.4 | Benzimidazolium salt **1d**

Purification by flash chromatography (dichloromethane: methanol = 10:1): a black solid, mp 228.3°C to 230.2°C; $^1$H NMR (400 MHz, DMSO-$d_6$): $\delta$ 10.55 (s, 1H), 8.51–8.58 (m, 2H), 8.44 (t, $J$ = 8.0 Hz, 1H), 8.36–8.26 (m, 3H), 7.96–7.89 (m, 2H), 7.84–7.75 (m, 2H), 7.53 (t, $J$ = 6.8 Hz, 1H), 7.39–7.34 (m, 1H), 4.87 (t, $J$ = 6.8 Hz, 2H), 3.13 (t, $J$ = 6.4 Hz, 2H). $^{13}$C NMR (100 MHz, DMSO-$d_6$): $\delta$ 171.92, 152.79, 144.92, 143.15, 143.10, 138.87, 138.00, 131.59, 129.47, 128.73, 127.68, 127.28, 126.08, 123.33, 121.68, 115.11, 114.59, 114.47, 113.99, 113.64, 43.31, 33.03. IR: (KBr) 3393, 2989, 1725, 1588, 1557, 1458, 1344,

1245, 1184, 1108, 1008, 796, 749 $cm^{-1}$. HRMS: (ESI-TOF), *m/z* calcd.: 384.1455 for $C_{22}H_{18}N_5O_2$; found: 384.1448 $[M - I]^+$. The NMR spectra and FT-IR spectra of benzimidazolium salt **1d** can be found in Figures S4 and S35.

### 4.2.5 | Benzimidazolium salt **1e**

Purification by flash chromatography (dichloromethane: methanol = 10:1): a white solid, mp 242.2°C to 243.3°C; $^1H$ NMR (400 MHz, DMSO-$d_6$): $\delta$ 12.73 (s, 1H), 10.57 (s, 1H), 8.61 (t, $J = 4.4$ Hz, 2H), 8.46 (t, $J = 8.0$ Hz, 1H), 8.37 (d, $J = 7.6$ Hz, 1H), 8.31 (t, $J = 8.4$ Hz, 2H), 7.96 (d, $J = 8.0$ Hz, 1H), 7.90 (d, $J = 7.6$ Hz, 1H), 7.85–7.77 (m, 2H), 7.56–7.52 (m, 1H), 7.40–7.36 (m, 1H),4.87 (t, $J = 6.8$ Hz, 2H), 3.16 (t, $J = 6.8$ Hz, 2H). $^{13}C$ NMR (100 MHz, DMSO-$d_6$): $\delta$ 171.77, 152.83, 144.96, 143.17, 138.91, 138.03, 131.61, 129.51, 128.74, 127.69, 127.28, 126.12, 123.36, 121.72, 115.13, 114.60, 114.48, 114.03, 113.70, 43.11, 32.81. IR: (KBr) 3393, 2998, 1733, 1596, 1557, 1474, 1397, 1360, 1245, 1184, 1092, 749 $cm^{-1}$. HRMS: (ESI-TOF), *m/z* calcd.: 384.1455 for $C_{22}H_{18}N_5O_2$; found: 384.1451 $[M - Br]^+$. The NMR spectra and FT-IR spectra of benzimidazolium salt **1e** can be found in Figures S5 and S36.

### 4.2.6 | Benzimidazolium salt **1f**

Purification by flash chromatography (dichloromethane: methanol = 10:1): a red solid, mp 194.6°C to 195.7°C; $^1H$ NMR (400 MHz, DMSO-$d_6$): $\delta$ 12.72 (s, 1H), 10.20 (s, 1H), 9.19 (s, 1H), 8.63 (s, 1H), 8.46 (t, $J = 8.0$ Hz, 1H), 8.28 (d, $J = 8.4$ Hz, 1H), 8.17 (d, $J = 8.0$ Hz, 1H), 8.12 (t, $J = 2.0$ Hz, 1H), 8.01 (d, $J = 8.0$ Hz, 1H), 7.81 (d, $J = 8.0$ Hz, 1H), 7.48–7.34 (m, 2H), 4.55 (t, $J = 6.8$ Hz, 2H), 3.06 (t, $J = 6.8$ Hz, 2H). $^{13}C$ NMR (100 MHz, DMSO-$d_6$): $\delta$ 172.18, 149.20, 145.84, 144.81, 144.37, 143.17, 136.34, 131.83, 125.09, 124.46, 124.07, 120.62, 119.84, 115.54, 114.17, 112.04, 46.02, 34.05. IR: (KBr) 3332, 3012, 1725, 1596, 1540, 1458, 1306, 1245, 1092, 796, 735 $cm^{-1}$. HRMS: (ESI-TOF), *m/z* calcd.: 334.1299 for $C_{18}H_{16}N_5O_2$; found: 334.1299 $[M - I]^+$. The NMR spectra and FT-IR spectra of benzimidazolium salt **1f** can be found in Figures S6 and S37.

### 4.2.7 | Benzimidazolium salt **1g**

Purification by flash chromatography (dichloromethane: methanol = 10:1): a yellow solid, mp 203.2°C to 203.5°C; $^1H$ NMR (400 MHz, DMSO-$d_6$): $\delta$ 10.64 (s, 1H), 8.77 (d, $J = 2.4$ Hz, 1H), 8.54 (dd, $J = 7.2$ Hz, $J = 2.4$ Hz, 1H), 8.44 (t, $J = 8.0$ Hz, 1H), 8.27 (dd, $J = 6.4$ Hz, $J = 2.4$ Hz, 1H), 8.15 (d, $J = 8.4$ Hz, 1H), 8.02 (d, $J = 8.0$ Hz, 1H), 7.95 (d, $J = 1.6$ Hz, 1H), 7.86–7.79 (m, 2H), 6.71 (dd, $J = 2.4$ Hz, $J = 1.6$ Hz, 1H), 4.61 (t, $J = 7.2$ Hz, 2H), 2.06 (hex, $J = 7.2$ Hz, 2H), 1.02 (t, $J = 7.2$ Hz, 3H). $^{13}C$ NMR (100 MHz, DMSO-$d_6$): $\delta$ 150.12, 145.73, 143.69, 143.32, 142.58, 131.69, 129.27, 128.04, 127.21, 115.71, 114.20, 113.99, 112.57, 109.18, 48.79, 22.05, 10.78. IR: (KBr) 3126, 3071, 1614, 1554, 1470, 1391, 1306, 1246, 1092, 1041, 930, 804, 767 $cm^{-1}$. The NMR spectra and FT-IR spectra of benzimidazolium salt **1g** can be found in Figures S7 and S38.

### 4.2.8 | Benzimidazolium salt **1h**

Purification by flash chromatography (dichloromethane: methanol = 10:1): a yellow solid, mp 199.6°C to 203.2°C; $^1H$ NMR (400 MHz, DMSO-$d_6$): $\delta$ 12.67 (s, 1H), 8.61–8.52 (m, 1H), 8.45 (t, $J = 8.0$ Hz, 1H), 8.28–8.26 (m, 1H), 8.23–8.20 (m, 1H), 8.01–7.90 (m, 1H), 7.85–7.79 (m, 1H), 7.76–7.64 (m, 2H), 6.66 (dd, $J = 2.8$ Hz, $J = 1.6$ Hz, 1H), 4.81 (t, $J = 6.8$ Hz, 2H), 4.05–4.00 (m, 1H), 3.00 (s, 3H), 1.99–1.75 (m, 1H), 1.24–1.15 (m, 1H). $^{13}C$ NMR (100 MHz, DMSO-$d_6$): $\delta$ 171.77, 152.74, 150.95, 143.95, 143.82, 143.31, 130.63, 130.61, 127.71, 127.12, 126.71, 119.29, 114.10, 113.73, 113.35, 109.19, 41.49, 32.42, 12.18. IR: (KBr) 3386, 2936, 1565, 1458, 1390, 1253, 1039, 940, 727, 658 $cm^{-1}$. HRMS: (ESI), *m/z* calcd.: 348.1455 for $C_{19}H_{18}N_5O_2$; found: 348.1448 $[M - I]^+$. The NMR spectra and FT-IR spectra of benzimidazolium salt **1h** can be found in Figures S8 and S39.

### 4.2.9 | Benzimidazolium salt **1i**

Purification by flash chromatography (dichloromethane: methanol = 10:1): a yellow solid, mp 207.5°C to 209.8°C; $^1H$ NMR (400 MHz, DMSO-$d_6$): $\delta$ 12.69 (s, 1H), 10.49 (s, 1H), 8.80–8.79 (m, 1H), 8.49–8.45 (m, 1H), 8.32–8.24 (m, 2H), 8.06–8.04 (d, $J = 8.4$ Hz, 1H), 7.82–7.72 (m, 3H), 4.81 (t, $J = 6.4$ Hz, 2H), 3.12 (t, $J = 6.8$ Hz, 2H). $^{13}C$ NMR (100 MHz, DMSO-$d_6$): $\delta$ 171.67, 149.50, 147.26, 142.78, 140.63, 131.58, 129.40, 127.67, 127.15, 125.17, 117.08, 115.82, 114.27, 43.03, 32.79. IR: (KBr) 3332, 2987, 1744, 1693, 1540, 1475, 1439, 1338, 1261, 1160, 780, 735 $cm^{-1}$. The NMR spectra and FT-IR spectra of benzimidazolium salt **1i** can be found in Figures S9 and S40.

#### 4.2.10 | Benzimidazolium salt **1j**

Purification by flash chromatography (dichloromethane: methanol = 10:1): a yellow solid, mp 152.1°C to 153.4°C; $^1$H NMR (400 MHz, DMSO-$d_6$): $\delta$ 9.78 (s, 1H), 8.13–8.10 (m, 1H), 8.02–8.00 (m, 1H), 7.71–7.66 (m, 2H), 4.68 (t, $J$ = 6.4 Hz, 2H), 4.09 (s, 3H), 2.99 (t, $J$ = 6.4 Hz, 2H). $^{13}$C NMR (100 MHz, DMSO-$d_6$): $\delta$ 172.22, 143.61, 132.16, 131.32, 126.99, 126.91, 114.14, 114.07, 43.02, 33.87, 33.45. IR: (KBr) 3332, 3080, 1725, 1698, 1558, 1458, 1386, 1353, 1245, 1153, 758, 735 cm$^{-1}$. The NMR spectra and FT-IR spectra of benzimidazolium salt **1j** can be found in Figures S10 and S41.

### 4.3 | General procedure for the synthesis of cyclic carbonates

Epoxides (5.0 mmol), **1a** (2 mol%), $CrCl_2$ (1.5 mol%), and TBAB (5 mol%) were successively put into a 25-ml Schlenk flask. The reaction mixture was stirred at 50°C for 24 h under a $CO_2$ atmosphere (1 atm, using a balloon). After the reaction was completed, the reactor was cooled to room temperature, and excess $CO_2$ was carefully vented off and 50-ml sodium chloride solution was added to quench reaction. The mixture was diluted with dichloromethane (20 ml), followed by extraction three times (3 × 20 ml) with dichloromethane. The solvent was removed under reduced pressure, and the products were isolated by flash chromatography. $^1$H NMR and $^{13}$C NMR spectra of cyclic carbonate **3a–p** can be found in Figures S11–S26.


## ACKNOWLEDGMENTS

We thank the support from Xinjiang Bingtuan Young and Middle-Aged Leading Scientists Program (2020CB027), Shihezi Young and Middle-Aged Leading Scientists Program (2019RC01), and the Open Sharing Fund for the Large-scale Instruments and Equipments of Shihezi University.


## AUTHOR CONTRIBUTIONS

**Kuikui Zhang:** Conceptualization; data curation; formal analysis; investigation; methodology; software. **Zhenbang Liu:** Data curation; investigation; software. **Ning Liu:** Conceptualization; data curation; formal analysis; methodology; software; supervision.

## CONFLICT OF INTEREST

The authors declare no competing financial interest.

## DATA AVAILABILITY STATEMENT

The data that support the findings of this study are available in the supporting information of this article.


## ORCID

*Kuikui Zhang* https://orcid.org/0000-0003-4320-0603
*Zhenbang Liu* https://orcid.org/0000-0003-0773-8668
*Ning Liu* https://orcid.org/0000-0001-7299-0400


## REFERENCES


[1] a) J. Klankermayer, S. Wesselbaum, K. Beydoun, W. Leitner, *Angew. Chem., Int. Ed.* **2016**, *55*, 7296; b) J. Rintjema, A. W. Kleij, *Synthesis* **2016**, *48*, 3863.

[2] H.-R. Li, L.-N. He, *Organometallics* **2020**, *39*, 1461.

[3] a) Y. Yuan, Y. Xie, D. Song, C. Zeng, S. Chaemchuen, C. Chen, F. Verpoort, *Appl. Organometal. Chem.* **2017**, *31*, e3867; b) A. Liu, J. Zhang, X. Lv, *Chin. J. Catal.* **2018**, *39*, 1320; c) Q. Liu, S. Lei, L. Ning, *Chin. J. Org. Chem.* **2019**, *39*, 2882.

[4] a) F. Della Monica, B. Maity, T. Pehl, A. Buonerba, A. De Nisi, M. Monari, A. Grassi, B. Rieger, L. Cavallo, C. Capacchione, *ACS Catal.* **2018**, *8*, 6882; b) V. Laserna, G. Fiorani, C. J. Whiteoak, E. Martin, E. Escudero-Adán, A. W. Kleij, *Angew. Chem., Int. Ed.* **2014**, *53*, 10416.

[5] a) J. L. S. Milani, A. M. Meireles, W. A. Bezerra, D. C. S. Martins, D. Cangussu, R. P. das Chagas, *ChemCatChem* **2019**, *11*, 4393; b) J. L. S. Milani, A. M. Meireles, B. N. Cabral, W. de Almeida Bezerra, F. T. Martins, D. C. da Silva Martins, R. P. das Chagas, *J. CO2. Util.* **2019**, *30*, 100.

[6] a) X.-B. Lu, B. Liang, Y.-J. Zhang, Y.-Z. Tian, Y.-M. Wang, C.-X. Bai, H. Wang, R. Zhang, *J. Am. Chem. Soc.* **2004**, *126*, 3732; b) C.-X. Miao, J.-Q. Wang, Y. Wu, Y. Du, L.-N. He, *ChemSusChem* **2008**, *1*, 236.

[7] a) R. L. Paddock, S. T. Nguyen, *J. Am. Chem. Soc.* **2001**, *123*, 11498; b) J. A. Castro-Osma, K. J. Lamb, M. North, *ACS Catal.* **2016**, *6*, 5012.

[8] a) C. J. Whiteoak, N. Kielland, V. Laserna, E. C. Escudero-Adán, E. Martin, A. W. Kleij, *J. Am. Chem. Soc.* **2013**, *135*, 1228; b) W.-M. Ren, Y. Liu, X.-B. Lu, *J. Org. Chem.* **2014**, *79*, 9771.

[9] F. Chen, T. Dong, T. Xu, X. Li, C. Hu, *Green Chem.* **2011**, *13*, 2518.

[10] a) R. Ma, L.-N. He, Y.-B. Zhou, *Green Chem.* **2016**, *18*, 226; b) C. Maeda, J. Shimonishi, R. Miyazaki, J.-y. Hasegawa, T. Ema, *Chem. – Eur. J.* **2016**, *22*, 6556.

[11] a) T. Ema, Y. Miyazaki, J. Shimonishi, C. Maeda, J.-y. Hasegawa, *J. Am. Chem. Soc.* **2014**, *136*, 15270; b) C. Maeda, T. Taniguchi, K. Ogawa, T. Ema, *Angew. Chem., Int. Ed.* **2015**, *54*, 134.

[12] a) M. H. Anthofer, M. E. Wilhelm, M. Cokoja, I. I. E. Markovits, A. Pöthig, J. Mink, W. A. Herrmann, F. E. Kühn, *Catal. Sci. Technol.* **2014**, *4*, 1749; b) Y.-B. Wang, Y.-M. Wang, W.-Z. Zhang, X.-B. Lu, *J. Am. Chem. Soc.* **2013**, *135*, 11996; c) W. Desens, T. Werner, *Adv. Synth. Catal.* **2016**, *358*, 622.

[13] a) A. Mirabaud, J.-C. Mulatier, A. Martinez, J.-P. Dutasta, V. Dufaud, *ACS Catal.* **2015**, *5*, 6748; b) T. Ema, K. Fukuhara, T. Sakai, M. Ohbo, F.-Q. Bai, J.-y. Hasegawa, *Catal. Sci. Technol.* **2015**, *5*, 2314.

[14] a) H. Zhou, G.-X. Wang, W.-Z. Zhang, X.-B. Lu, *ACS Catal.* **2015**, *5*, 6773; b) Q.-W. Song, L.-N. He, J.-Q. Wang, H. Yasuda, T. Sakakura, *Green Chem.* **2013**, *15*, 110.
[15] Y. Toda, Y. Komiyama, A. Kikuchi, H. Suga, *ACS Catal.* **2016**, *6*, 6906.
[16] M. Cokoja, M. E. Wilhelm, M. H. Anthofer, W. A. Herrmann, F. E. Kühn, *ChemSusChem* **2015**, *8*, 2436.
[17] J.-W. Huang, M. Shi, *J. Org. Chem.* **2003**, *68*, 6705.
[18] L. Longwitz, J. Steinbauer, A. Spannenberg, T. Werner, *ACS Catal.* **2018**, *8*, 665.
[19] F. Wu, Y. Lin, *Appl. Organometal. Chem.* **2020**, *34*, e5427.
[20] a) C.-B. Bo, Q. Bu, X. Li, G. Ma, D. Wei, C. Guo, B. Dai, N. Liu, *J. Org. Chem.* **2020**, *85*, 4324; b) W.-Y. Song, Q. Liu, Q. Bu, D. Wei, B. Dai, N. Liu, *Organometallics* **2020**, *39*, 3546; c) J.-B. Shi, Q. Bu, B.-Y. Liu, B. Dai, N. Liu, *J. Org. Chem.* **2021**, *86*, 1850.
[21] F. Chen, D. Chen, L. Shi, N. Liu, B. Dai, *J. CO2. Util.* **2016**, *16*, 391.
[22] Y.-B. Wang, B.-Y. Liu, Q. Bu, B. Dai, N. Liu, *Adv. Synth. Catal.* **2020**, *362*, 2930.
[23] V. Caló, A. Nacci, A. Monopoli, A. Fanizzi, *Org. Lett.* **2002**, *4*, 2561.
[24] F. Esteve, B. Altava, M. I. Burguete, M. Bolte, E. García-Verdugo, S. V. Luis, *Green Chem.* **2020**, *22*, 4697.
[25] J. Hu, J. Ma, H. Liu, Q. Qian, C. Xie, B. Han, *Green Chem.* **2018**, *20*, 2990.
[26] H. Zhou, W.-Z. Zhang, C.-H. Liu, J.-P. Qu, X.-B. Lu, *J. Org. Chem.* **2008**, *73*, 8039.
[27] a) J. Sun, L. Han, W. Cheng, J. Wang, X. Zhang, S. Zhang, *ChemSusChem* **2011**, *4*, 502; b) J. A. Castro-Osma, J. Martínez, F. de la Cruz-Martínez, M. P. Caballero, J. Fernández-Baeza, J. Rodríguez-López, A. Otero, A. Lara-Sánchez, J. Tejeda, *Catal. Sci. Technol.* **2018**, *8*, 1981; c) N. Liu, Y.-F. Xie, C. Wang, S.-J. Li, D. Wei, M. Li, B. Dai, *ACS Catal.* **2018**, *8*, 9945.
[28] F. Chen, N. Liu, B. Dai, *ACS Sustainable Chem. Eng.* **2017**, *5*, 9065.

## SUPPORTING INFORMATION

Additional supporting information may be found online in the Supporting Information section at the end of this article.

**How to cite this article:** K. Zhang, Z. Liu, N. Liu, *Appl Organomet Chem* **2021**, e6347. https://doi.org/10.1002/aoc.6347